

Characterization of thermal-shock cracks in ceramic bars

XU XiangHong^{*}, TIAN Cheng, SHENG ShiLong, LIN ZhongKang & SONG Fan

State Key Laboratory of Nonlinear Mechanics (LNM), Institute of Mechanics, Chinese Academy of Sciences, Beijing 100190, China

Received May 29, 2014; accepted July 8, 2014; published online September 22, 2014

Experimental analysis of the cracking in the ceramics subsequent to water quenching have been conducted to clarify the uncertainties of cracking in the ceramics when subjected to thermal shock. The results here indicate that at the critical point of quench temperature, the crack density and the depth reached the minimum and the maximum limits, respectively. On increase of the quench temperature, the crack density increased rapidly before reaching its saturation point, while the crack depth initially decreased rapidly and then increased gradually before reaching its saturation point.

thermal-shock crack, ceramics

PACS number(s): 44.10.+I, 62.20.Mk, 65.40.-b, 65.40.De

Citation: Xu X H, Tian C, Sheng S L, et al. Characterization of thermal-shock cracks in ceramic bars. *Sci China-Phys Mech Astron*, 2014, 57: 2205–2208, doi: 10.1007/s11433-014-5562-6

1 Introduction

Cracking plays a key role in the loss of the strength in ceramics subjected to thermal-shock [1–5]. The characteristics of cracks generated by the changes of quench temperature are vital for understanding underlying mechanisms related to the thermal-shock. It is widely accepted that neither cracking nor residual strength undergo change at temperatures below the critical temperature, T_c , however, the strength is significantly decreased at T_c due to the cracks [3–9].

Till date, the contradictions regarding cracking and residual strength have been extensively investigated, especially when the temperature range is between T_c and the second critical temperature.

Hasselman's [4] unified theory of thermal-shock states that the crack depth, the crack density, and the residual strength would remain constant within a quench temperature interval. Bertsch et al. [6] demonstrated that the crack density generally increased with increase in the quench

temperature, leading to the lowest strength immediately above the T_c , while, further increase in the quench temperature, could gradually increase the crack density. Davidge et al. [7] found that the crack depth increased slowly, and the density of cracking increased rapidly at the onset before reaching a certain saturation value at the end. Bahr's [8] numerical simulation indicated that the crack depth exhibited a non-monotonic temperature dependence. Shao et al. [9] showed that both the depth and the density of long cracks gradually increased with temperature. In these investigations, however, thermal-shock cracks were inadequately characterized, and no consensus was found regarding the relationship between the crack evolution and the quench temperature.

In this study, experiments were performed with the thermal-shock cracks. In comparison with previous work, we could resolve the current uncertainties of cracking by the thermal-shock.

2 Experimental procedure

Commercially available Al_2O_3 powder (particle size 0.5 μm ,

^{*}Corresponding author (email: xxh@lnm.imech.ac.cn)

purity 99.5%) was compressed into blocks at 20 MPa and subsequently sintered at 1650°C for 2 h at normal pressure. The sintered bodies, with 4% porosity and 10 μm mean grain size, were cut into bars with dimensions of 50 mm \times 9.8 mm \times 5 mm. The ceramic bars were ground, polished, slightly chamfered, and then stacked as shown in Figure 1 to prevent coolant from accessing the interior surfaces.

The stacks were initially heated to a pre-determined temperature ranging between 200°C to 800°C in a muffle furnace, for 20 min, and then quenched in water at 17°C. After drying, the quenched samples were immersed in dye and then wiped with absorbent cotton. The crack patterns of each sample after quenching were thus distinguishable and were photographed by a digital scanner (Figure 2).

The crack density and the crack depth were determined to characterize the complex cracks on the interior surface. The number of cracks per unit length along the lengthwise direction was defined as crack density. The maximum vertical distance from the tip of a crack to the side was defined as crack depth and its dimensionless expression was obtained by dividing by half the sample height (4.9 mm). With subsequent observation and statistical analysis, cracks with depth greater and lesser than 0.42 were defined as the long and short cracks respectively. The density and depth of long and short cracks with respect to the quench temperatures are

shown in Figures 3 and 4. To remove boundary effects, 5 mm sections near each end of the ceramic bars were excluded from the statistical range. For each temperature, five samples were selected to measure and analyze the crack characteristics for proper sample dispersion.

3 Results and discussion

No crack was detected with the dye-penetrant method at the quenching temperature of $T < 220^\circ\text{C}$. However, cracks were detected at the higher temperatures (Figure 2). The critical temperature, T_c suggested that the thermal-shock crack occurred first at 220°C. As the quench temperature increased, the generation of the thermal-shock cracks exhibit three

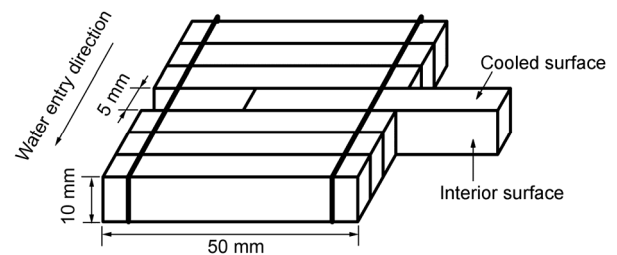


Figure 1 Stack of samples prepared for thermal shock test. Arrows indicated cooled surface and interior surface of the bars.

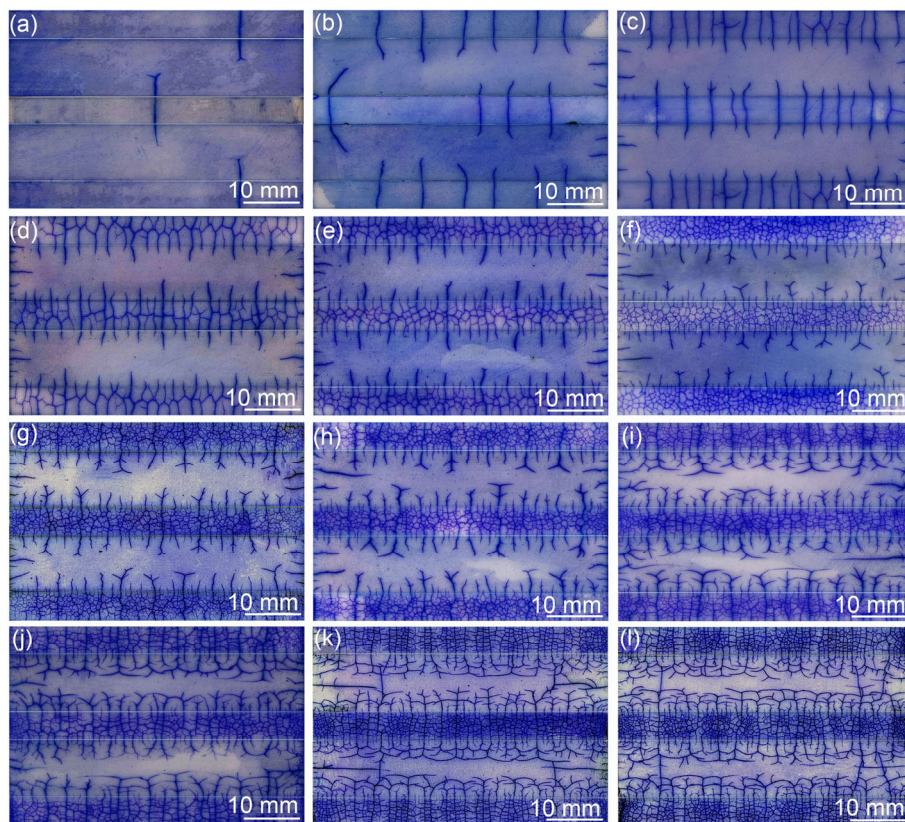


Figure 2 (Color online) Thermal shock crack patterns made visible by blue ink on interior faces (wide strips) and cooled surface (narrow strips) of the stacked samples quenched in water at 17°C. The quenching temperature T is (a) 220°C; (b) 230°C; (c) 260°C; (d) 280°C; (e) 320°C; (f) 350°C; (g) 380°C; (h) 400°C; (i) 500°C; (j) 600°C; (k) 700°C and (l) 800°C, respectively.

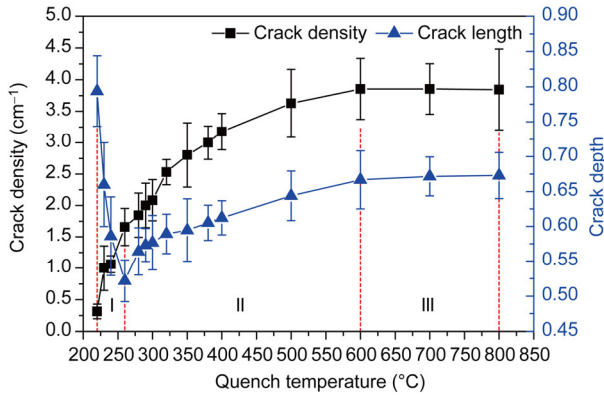


Figure 3 (Color online) Density and depth of long crack as functions of quench temperature. The values are the statistical averages and error bars of five samples.

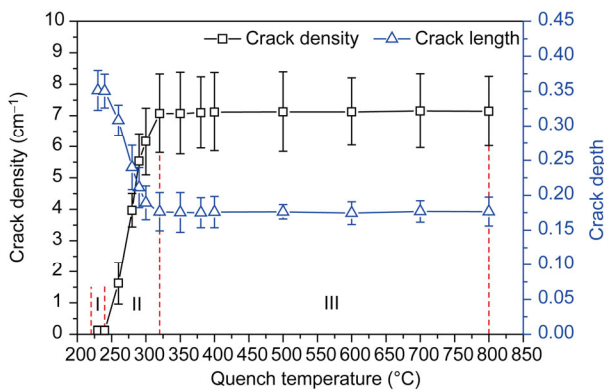


Figure 4 (Color online) Density and depth of short crack as functions of quench temperature. The values are the statistical averages and error bars of five samples.

main features; the density and depth of cracks were changed, a hierarchical structure of long and short cracks was formed, and bifurcations and multiple bifurcations appeared.

Long crack density and depth versus the quench temperature, divided into three stages have been illustrated in Figure 3. The crack density exhibited a rapid growth, a slow growth, and a steady state, while the crack depth followed a rapid decrease, a slow growth, and a steady state. In the first stage, i.e., $T_c \leq T < 260^\circ\text{C}$, the crack density increased and the crack depth decreased. At the critical temperature, T_c , only one or two sparse long cracks appear with low density (0.31 cm^{-1}), while the crack depth reaches the maximum value of 0.79. At the quench temperature of $T = 260^\circ\text{C}$, the density increases to 1.7 cm^{-1} with a mean growth rate of $3.4 \times 10^{-2}\text{ (cm}\cdot^\circ\text{C)}^{-1}$, and the depth decreases to the minimum value of 0.52 with a growth rate of $-6.8 \times 10^{-3}\text{ }^\circ\text{C}^{-1}$. In the second stage, i.e., when $260^\circ\text{C} \leq T < 600^\circ\text{C}$, both the density and the depth increase gradually. At the quench temperature of $T = 600^\circ\text{C}$, the density increases to 3.9 cm^{-1} with a growth rate of $6.5 \times 10^{-3}\text{ (cm}\cdot^\circ\text{C)}^{-1}$, and the depth increases to 0.67 with a mean growth rate of $4.4 \times 10^{-4}\text{ }^\circ\text{C}^{-1}$.

In the third stage, i.e., with $600^\circ\text{C} \leq T \leq 800^\circ\text{C}$, both the density and depth almost remained unchanged.

The short crack density and depth versus the quench temperature also experiences three stages (Figure 4). In the first stage, i.e., when $230^\circ\text{C} \leq T \leq 240^\circ\text{C}$, the crack density and depth are almost unchanged and no short cracks appear at T_c . At the quench temperature of $T = 230^\circ\text{C}$, sparse short cracks appear at a low density of 0.13 cm^{-1} , with the maximum depth of 0.35. In the temperature range from 240°C to 320°C , these two values are almost unchanged. In the second stage, i.e., when $240^\circ\text{C} < T < 320^\circ\text{C}$, the short crack density increases rapidly while the short crack depth decreases. At the quench temperature of $T = 320^\circ\text{C}$, the density increases to 7.1 cm^{-1} with a mean growth rate of $7.7 \times 10^{-2}\text{ (cm}\cdot^\circ\text{C)}^{-1}$, and the depth decreases to the minimum value of 0.18 with a mean growth rate of $-1.9 \times 10^{-3}\text{ }^\circ\text{C}^{-1}$. In the third stage, i.e., with $320^\circ\text{C} \leq T \leq 800^\circ\text{C}$, both the density and the depth are nearly constant.

Absence of short cracks accompanied by only a few long cracks with obvious bifurcations can be observed at T_c , despite the fact that the long crack depth already reaches the maximum value in the crack series (Figure 2(a)). When the quench temperature is increased, the long crack depth decreases rapidly, and the density increases rapidly. A small number of the short cracks appear as the temperature is increased to 230°C . The boundary between the long and the short cracks is non-distinguishable (Figure 2(b)). At the quench temperature of $T = 260^\circ\text{C}$, the long crack depth grows to the minimum value and the boundary between the long and the short cracks becomes more fuzzy. Similarly, the short crack depth decreases as rapidly as the density increases. The reduction of the long crack depth is 3.6 times faster than that of the short one. The increase of the long crack density is only 0.5 times lower than that of the short crack density (Figure 2(c)). Furthermore, the long crack depth increases gradually and the growth rate is only 6.5% of the absolute growth rate from the previous stage. The long crack density growth also is slow down, which is at a growth rate of only 19% of that in the previous stage. The short crack depth continuously drops while the short crack density rapidly grows. The long and the short crack classification become increasingly evident. The bifurcation gradually disappears (Figure 2(d)). At the quench temperature of $T = 320^\circ\text{C}$, the short crack density reaches the maximum value and the crack depth achieves the minimum one, and both of them remain constant thereafter as the quench temperature is increased. Moreover, the bifurcation reappears (Figure 2(e)), and the length of the bifurcation along the lateral direction increases. Meanwhile, the multiple bifurcations appear in the vertical direction as the temperature increases (Figures 2(f)–(l)). At the quench temperature $T = 600^\circ\text{C}$, the long crack density and the depth reach the saturation and then maintain different saturation values as the quench temperature is continuously raised. Clearly, in the

high quench temperature region, the crack density and the depth achieve a saturation, while the bifurcations become connected and the energy consumptive (Figures 2(j)–(l)).

4 Conclusions

The crack density increases rapidly when the quench temperature is higher than a critical temperature, but eventually approaches a saturation value with increasing the quench temperature. The rapid growth period includes the quick formation of the long cracks, followed by the short ones. The density of the short cracks reaches saturation at a much lower temperature (less than about 280°C) than that of the long cracks.

Similar to the crack density, the crack depth also reaches a saturation as the quench temperature increased to a certain value in spite of the fact that the saturation value of the short crack depth occurred at a much lower temperature than that of the long cracks. However, with increasing the quench temperature to be higher than the critical temperature, the crack depth experiences a period of decrease, which is slightly different from the evolution of the crack density. Subsequently, the short crack depth instantaneously reaches the saturation, sometimes even before 280°C, while the long crack depth first increases slowly and then approaches the saturation.

The contrary evidences in previous research on cracking and the residual strength were related to the different quench temperature ranges and very large temperature intervals. Davidge and Shao [7,9] did not show a decrease in the crack depth after the critical temperature for the reason that their experiments did not focus on the temperature intervals beyond the critical temperature of T_c . Bertsch and Shao [6,9] demonstrated that the crack density and depth increased gradually with increasing the quench temperature,

however, saturation was not attained as their experiments were not conducted at higher temperatures. Bertsch and Bahr [6,8] found that the crack depth exhibited non-monotonic dependence on quench temperature while the depreciative characteristics of crack depth beyond the critical temperature, and the crack depth evolution trend thereafter were not quantified.

This work was supported by the National Natural Science Foundation of China (Grant Nos. 11023001 and 11272313).

- 1 Salvini V R, Pandolfelli V C, Bradt R C. Extension of Hasselman's thermal shock theory for crack/microstructure interactions in refractories. *Ceram Int*, 2012, 38(7): 5369–5375
- 2 Pompe W E. Thermal shock behavior of ceramic materials-modeling and measurement. In: Schneider G A, Petzow G, eds. *Thermal Shock and Thermal Fatigue Behavior of Advanced Ceramics*. Netherlands: Kluwer Academic Publishers, 1993. 3–14
- 3 Song F, Meng S H, Xu X H, et al. Enhanced thermal shock resistance of ceramic through biomimetically inspired nanofins. *Phys Rev Lett*, 2010, 104(12): 125502
- 4 Hasselman D P H. Unified theory of thermal shock fracture initiation and crack propagation in brittle ceramics. *J Am Ceram Soc*, 1969, 52(11): 600–604
- 5 Wang B L, Han J C. Fracture mechanics associated with non-classical heat conduction in thermoelastic media. *Sci China-Phys Mech Astron*, 2012, 55: 493–504
- 6 Bertsch B E, Larson D R, Hasselman D P H. Effect of crack density on strength loss of polycrystalline Al_2O_3 subjected to severe thermal shock. *J Am Ceram Soc*, 1974, 57(5): 235–236
- 7 Davidge R W, Tappin G. Thermal shock and fracture in ceramics. *Trans Brit Ceram Soc*, 1967, 66(8): 405–422
- 8 Bahr H A, Weiss H J, Maschke H G, et al. Multiple crack propagation in a strip caused by thermal shock. *Theor Appl Fract Mech*, 1988, 10(3): 219–226
- 9 Shao Y F, Zhang Y, Xu X H, et al. Effect of crack pattern on the residual strength of ceramics after quenching. *J Am Ceram Soc*, 2011, 94(9): 2804–2807